ChemSusChem

Research Article
doi.org/10.1002/cssc.202200241

Chemistry Europe
European Chemical Societies Publishing

www.chemsuschem.org

Integrated Cascade Process for the Catalytic Conversion of 5-Hydroxymethylfurfural to Furanic and TetrahydrofuranicDiethers as Potential Biofuels

Sara Fulignati,[a] Claudia Antonetti,[a, b] Tommaso Tabanelli,[c] Fabrizio Cavani,[c] and Anna Maria Raspolli Galletti*[a]

The depletion of fossil resources is driving the research towards alternative renewable ones. Under this perspective, 5-hydroxymethylfurfural (HMF) represents a key molecule deriving from biomass characterized by remarkable potential as platform chemical. In this work, for the first time, the hydrogenation of HMF in ethanol was selectively addressed towards 2,5-bis(hydroxymethyl)furan (BHMF) or 2,5-bis(hydroxymethyl)tetrahydrofuran (BHMTHF) by properly tuning the reaction conditions in the presence of the same commercial catalyst (Ru/C), reaching the highest yields of 80 and 93 mol%, respectively. These diols represent not only interesting monomers but strategic precursors for two scarcely investigated ethoxylated biofuels, 2,5-bis(ethoxymethyl)furan (BEMF) and 2,5-bis(ethoxymethyl)tetrahydrofuran (BEMTHF). Therefore, the etherification with ethanol of pure BHMF and BHMTHF and of crude BHMF, as obtained from hydrogenation step, substrates scarcely investigated in the literature, was performed with several commercial heterogeneous acid catalysts. Among them, the zeolite HZSM-5 (Si/Al = 25) was the most promising system, achieving the highest BEMF yield of 74 mol%. In particular, for the first time, the synthesis of the fully hydrogenated diether BEMTHF was thoroughly studied, and a novel cascade process for the tailored conversion of HMF to the diethyl ethers BEMF and BEMTHF was proposed.

Introduction

The depletion of fossil fuels and their impact on the environmental pollution is driving the world forces towards the partial substitution of them with significant amount of biofuels, which should represent 32% of gross final consumption of energy within 2030.[1] Therefore, the valorization of lignocellulosic biomass is a theme of paramount relevance. Under this perspective, 5-hydroxymethylfurfural (HMF) represents a very important molecule, being precursor of several monomers,[2] solvents,[2] adhesive,[3] surfactant,[4] and biofuels such as 2,5-dimethylfuran, 5-(alkoxymethyl)furfurals, and 2,5-bis(alkoxymethyl)furans.[5] Among them, the ethers have attracted great attention because they can be blended with fossil diesel without causing problems for the engine performance, also reducing the particulate emissions.[6] Up to now, 5-(ethoxymethyl)furfural (EMF) is the most studied, having a boiling point comparable to diesel fuel (235 °C), low toxicity, and an energy density of 30.3 MJ L^{-1}, which is only 10% lower than that of commercial diesel.[6b,7] In the literature, the etherification of HMF to EMF has been performed in the presence of both homogeneous and heterogeneous acid catalysts (Table S1), and both strength and type of acidity markedly influenced the reaction. In fact, the strong Lewis acidity promoted the direct etherification of HMF, while the Brønsted acidity promoted the EMF formation through the acetalization, thus the acetal 5-(hydroxymethyl)-2-(diethoxymethyl)furan (HMFDA) could be observed together with the alcoholysis product ethyl levulinate (EL).[8] However, the aldehydic group present in the chemical structure of EMF causes low chemical stability and makes it miscible with commercial diesel only up to 25 vol%.[6b,8,9] On the other hand, the 2,5-bis(alkoxymethyl)furans (BAMFs) appear more promising biofuels with higher stability and greater blending properties in commercial diesel due to the absence of the aldehydic group. In particular, 2,5-bis(ethoxymethyl)furan (BEMF) is very attractive because it has higher energy density (30.8 MJ L^{-1}), higher boiling point (215 °C), and lower water solubility than ethanol, which is one of the main biomass-derived biofuels. Moreover, it is characterized by a higher cetane number than that of the commercial

[a] Dr. S. Fulignati, Prof. C. Antonetti, Prof. A. M. Raspolli Galletti
Department of Chemistry and Industrial Chemistry
University of Pisa
via Giuseppe Moruzzi 13,
56124, Pisa (Italy)
E-mail: anna.maria.raspolli.galletti@unipi.it
[b] Prof. C. Antonetti
Interuniversity Consortium for Chemical Reactivity and Catalysis (CIRCC)
Via CelsoUlpiani 27, 70126,
Bari (Italy)
[c] Dr. T. Tabanelli, Prof. F. Cavani
Department of Industrial Chemsistry "TosoMontanari"
Alma Mater Studiorum University of Bologna
Viale Risorgimento 4, 40136,
Bologna (Italy)

Supporting information for this article is available on the WWW under https://doi.org/10.1002/cssc.202200241

This publication is part of a collection of invited contributions focusing on "Green Conversion of HMF". Please visit chemsuschem.org/collections to view all contributions.

diesel (≈80 vs. ≈50 of diesel fuel), with similar flash point (59 °C) and cold filter plugging point (−21 °C). In addition, BEMF is completely miscible with commercial diesel giving blending mixtures with better combustion performances and lower emission of smoke, CO_2, NO_x, and SO_x.[9b,10] Regarding the synthesis of BEMF, analogously to the other BAMFs, it can be performed from HMF through two different reaction mechanisms (Scheme 1): route 1 is hydrogenation of HMF to 2,5-bis(hydroxymethyl)furan (BHMF) and its subsequent etherification to BEMF with 5-(ethoxymethyl)furfuryl alcohol (EMFA) as intermediate; route 2 is etherification of HMF to EMF, with subsequent reduction to EMFA and its final etherification into BEMF.[11] As is well-known, the etherification steps are catalyzed by acids.[12] Therefore, the second multi-step route may lead to the formation of larger amount of by-products because under acidic conditions HMF may also be converted to HMFDA and to EL, due to the presence of the strongly reactive aldehydic group.[12a] Therefore, route 1, involving the reduction of the aldehyde moiety as first step, appears more suitable in order to achieve higher selectivity toward the target product. Under harsher hydrogenation reaction conditions, the furanic ring could also be reduced, giving rise to the production of 2,5-bis(hydroxymethyl)tetrahydrofuran (BHMTHF) (Scheme 1), a very promising monomer for the synthesis of renewable polyurethanes and polyesters.[13]

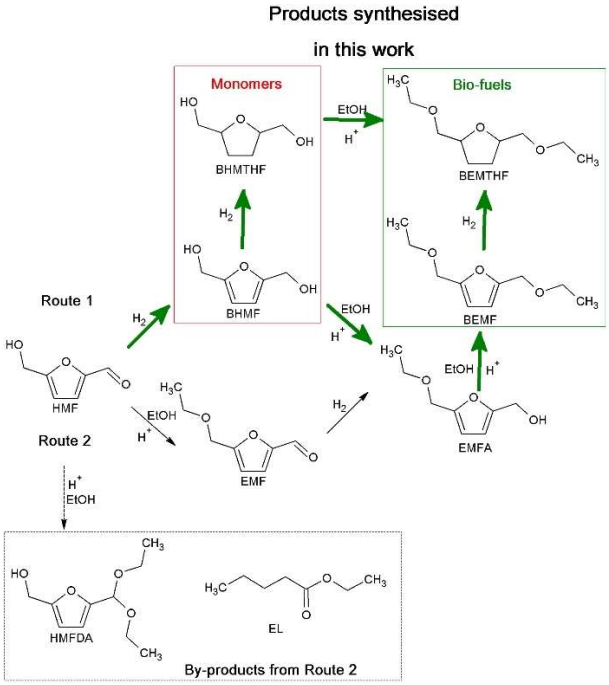

Scheme 1. Possible reaction pathways for the synthesis of BEMF from HMF and pathways of the cascade process for the selective synthesis of diol monomers (BHMF and BHMTHF) and biofuels (BEMF and BEMTHF) proposed in the present work (evidenced with green arrows).

In addition, analogously to BHMF, BHMTHF could also be etherified to give 2,5-bis(ethoxymethyl)tetrahydrofuran (BEMTHF), a reaction that, to the best of our knowledge, has not been yet deepened in the literature (Scheme 1). BEMTHF could be a novel potentially interesting biofuel because De Jong et al. found that hydrogenated furanics, such as 2-(ethoxymethyl)tetrahydrofuran, gave a better engine performance in terms of NO_x emission and maximum cylinder pressure than the unsaturated ones, such as 2-(ethoxymethyl)furan.[10b] In particular, the authors proposed the (alkoxymethyl)tetrahydrofuran ethers as aviation fuels due to their low melting point, high energy density, high flash point, and good miscibility with fossil fuels.[6a] On this basis and in order to perform the synthesis of fully renewable furanic/tetrahydrofuranic ethers from HMF in a cascade process, ethanol should be preferred as solvent for both the hydrogenation and the etherification steps, being one of the most important renewable alcohols. Regarding the HMF hydrogenation in ethanol, the synthesis of BHMF has been largely investigated mainly in the presence of ad-hoc synthesized catalysts, whose employment on large scale is still limited due to the cost of catalyst production together with the difficult reproducibility of catalyst formulation, aspects significantly more demanding and detrimental compared to commercially available systems. On the other hand, only few works reported the production of BHMTHF in ethanol (Table 1). Noble metal-based (Ru and Pd) catalysts preferably give BHMTHF as major product with the exception of platinum, which mainly reduces HMF to BHMF with good selectivity.[14] In fact, the synthesis of BHMF was generally carried out with catalysts having platinum or the non-noble

Table 1. Overview of the literature on the HMF hydrogenation carried out in ethanol.

Test	[HMF] [wt%]	Cat. (metal/HMF)	Diol product	*T* [°C]	*P* [bar]	*t* [h]	HMF conv. [mol%]	Yield [mol%]	Ref.
1	6.0	5 wt%Pt/Al_2O_3 (0.4)	BHMF	23	14	18	n.a.[a]	85	[15a]
2	3.2	0.1 wt%Pt/CZ[b] (0.1)	BHMF	170	10	8	100	97	[15b]
3	3.2	0.25 wt%Pt/CZ[b] (0.2)	BHMF	20	5	6	87	87	[15c]
4	3.2	20 wt% Cu/Al_2O_3 (4.0)	BHMF	70	50	3.5	99	98	[16a]
5	0.5	Cu@C-POP[c] (2.5)	BHMF	150	20	10	100	100	[16b]
6	n.a.[a]	3 wt% Cu/CZ[b] (n.a.[a])	BHMF	170	10	2	70	70	[16c]
7	0.8	7.6 wt% Cu-Al_2O_3 (3.8)	BHMF	130	30	1	100	93	[16d]
8	3.1	Cu20-PMO[d] (5.9)	BHMF	100	50	3	100	99	[16e]
9	3.1	CuZn alloy (18.6)	BHMF	120	70	3	100	95	[16f]
10	4.8	$Ru(OH)_x/ZrO_2$ (0.2)	BHMF	120	30	6	100	100	[17]
11	4.0	4 wt % Ru/$MnCo_2O_4$ (0.8)	BHMTHF	100	82	24	73	68	[18]
12	3.1	5 wt%Pd/Al_2O_3 (0.1)	BHMTHF	120	70	3	100	99	[16f]

[a] n.a. = not available. [b] Ceria–zirconia. [c] Copper supported on catechol-based organic polymer. [d] Copper (20 mol%)-doped porous metal oxide.

metal copper as active species (Table 1).[15,16] The etherification reaction is catalyzed by acids, thus the most investigated catalytic systems for pure BHMF conversion are commercial heterogeneous acid resins, in particular Amberlysts,[6b,19] but ad-hoc synthesized catalysts have also been adopted leading to very interesting yields of BEMF (higher than 80 mol%),[20] although their employment on large scale is still limited (Table 2). The heterogeneous systems are preferred because they are not only easier to be separated from the reaction mixture, but can also reduce the by-products formation, such as ethyl levulinate and diethyl ether, the latter deriving from the self-etherification of the solvent.[15a] In addition, in order to limit the by-products formation, generally the adopted temperatures were relatively low, below 80 °C, but long reaction times, higher than 3 h, were employed. Mostly, the synthesis of BEMF has been investigated starting from pure BHMF (Table 2), and very few works reported the employment of HMF as starting feedstock in a two-step cascade process involving HMF hydrogenation using the selected alcohol as reaction medium and successive etherification reagent. This cascade approach could be more interesting for future applications on larger scale because HMF is directly obtained from biomass.[21] In this sense, Balakrishnan et al. investigated the one-pot production of BEMF from HMF in ethanol employing 5 wt%Pt/Al_2O_3 as hydrogenating catalyst and Amberlyst-15 for the etherification.[15a] Under the optimal reaction conditions (60 °C; 14 bar of H_2; 18 h) the authors achieved the best BEMF yield of 59 mol% with respect to the starting HMF. On the other hand, Han et al. proposed a cascade approach: in the first step the authors carried out the hydrogenation of HMF to BHMF in the presence of $Ru(OH)_x$/ZrO_2 as catalyst reaching a complete yield of BHMF; subsequently the catalyst was separated and the obtained mixture was etherified employing Amberlyst-15 achieving a BEMF yield of 70 mol% working at 60 °C for 10 h.[19b] A cascade approach was also proposed by Elsayed et al., who performed the hydrogenation of HMF to BHMF through the Meerwein–Ponndorf–Verley transfer hydrogenation mechanism using ethanol as hydrogen donor and a magnetic bimetallic nanocatalyst (ZnO-Fe_3O_4/AC), achieving a BHMF yield of 60 mol% under the optimal reaction conditions (200 °C and 12 h).[19a] At the end of the first step, the catalyst was removed and replaced with the selected acid resin, chosen among Amberlyst-16, Amberlyte IR120, and Dowex 50WX2. The etherification was carried out with the different resins at 65 °C for 10 h and the obtained BEMF yields (expressed as area percent) were 65, 60, and 62 %, respectively.

The present work proposes a new cascade process aiming at the selective synthesis of two different diol monomers (BHMF and BHMTHF) and of the new-generation diether biofuels (BEMF and BEMTHF) starting from HMF (Scheme 1). Only commercial catalysts have been adopted in the involved reactions in order to allow a faster and cheaper scale-up. In particular, 5 wt%Ru/C was employed in the HMF hydrogenation step due to its efficiency in the same reaction performed in water.[14,22] On the other hand, the etherification of the pure BHMF and BHMTHF to BEMF and BEMTHF, respectively, has been studied testing different commercial acid heterogeneous catalysts, and the found optimal reaction conditions were adopted for the etherification of the crude mixtures deriving from the hydrogenation step, an aspect scarcely studied in the literature until now.[15a,19a,b] The synthesis of BEMTHF was studied also through a novel multistep process involving the hydrogenation of crude BEMF. To the best of our knowledge, the synthesis of BEMTHF has been reported for the first time in the present work, opening the way to the sustainable production of a new potential jet-fuel.

Results and Discussion

Hydrogenation of HMF to BHMF and BHMTHF

Starting from our previous study performed in water,[14] a preliminary hydrogenation test in ethanol was carried out adopting the same conditions resulted optimal for the synthesis of BHMTHF (100 °C and 50 bar H_2), and the results are reported in Table 3, where they are compared with those ascertained in aqueous medium. Despite the higher solubility of hydrogen in alcoholic medium than in water,[23] the conversion of HMF was slower in ethanol, in agreement with the literature,[18] reaching the complete conversion only after 120 min. However, already at incomplete HMF conversion (75.5 mol%, after 15 min) the BHMTHF yield was not negligible (14.7 mol%), showing that in ethanol the hydrogenation of furan ring was significant already at short reaction times. In addition, the reaction in ethanol was less selective towards the two diols, leading to a lower carbon balance upon prolonging the reaction time. In order to investigate the nature of the by-products, the samples collected

Table 2. Overview of the literature on the pure BHMF etherification to BEMF carried out in ethanol.

Test	[BHMF] [wt%]	Cat. (w_{BHMF}/w_{cat})	T [°C]	t [h]	BHMF conv. [mol%]	Yield [mol%]	Ref.
13	1.6	Amberlyst-15 (3.2)	60	3	100	50	[6b]
14	6.0	Amberlyst-15 (12.8)	40	16	n.a.[a]	80	[15a]
15	2.6	Amberlyst-15 (5.1)	60	10	100	70	[19b]
16	8.5	Purolite CT269DR (10.0)	40	24	n.a.[a]	99	[19c]
17	1.3	AT(0.50)-OT[b] (1.0)	80	12	100	95	[20a]
18	3.1	Glu-TSOH-Ti[c] (6.4)	80	8	n.a.[a]	92	[20b]
19	3.3	Ni_2P/SiO_2 (5.1)	150	3	100	80	[20c]

[a] n.a. = not available. [b] ZSM-5 subjected to an alkaline treatment (AT) with NaOH at 0.50 M followed by an oxalic acid treatment (OT). [c] Sulfonatedcarbocatalyst obtained from the hydrotreatment of glucose, *p*-toluenesulfonic acid, and titanium(IV) isopropoxide.

Table 3. Comparison of the HMF hydrogenation in ethanol and water[14] in the presence of 5 wt%Ru/C under the same reaction conditions.[a]

t [min]	HMF conv. [mol%]		BHMF yield [mol%]		BHMTHF yield [mol%]		Carbon balance[b] [mol%]	
	Run 1 (ethanol)	Ref. 14 (water)	Run 1 (ethanol)	Ref. 14 (water)	Run 1 (ethanol)	Ref. 14 (water)	Run 1 (ethanol)	Ref. 14 (water)
15	75.5	90.1	54.0	81.8	14.7	2.6	93.2	94.3
30	85.0	98.8	61.5	71.3	21.1	25.0	97.6	97.6
60	94.5	100	52.2	16.9	35.3	71.5	93.0	88.4
120	100	100	26.5	0.0	60.2	92.0	86.7	92.0
240	100	100	0.0	0.0	89.7	95.3	89.7	95.3

[a] Reaction conditions: Ru/HMF ratio = 1 wt%; $T = 100\,^{\circ}C$; $P = 50$ bar; [HMF] = 30 g L^{-1}. [b] Carbon balance = $[(mol_{unconvertedHMF} + mol_{BHMF} + mol_{BHMTHF})/mol_{startingHMF}] \times 100$.

during the reaction were analyzed through GC–MS, which allowed the identification of compounds deriving from hydrogenolysis, such as 5-methylfurfural (MF), 5-methylfurfurylalcohol (MFA), and 5-methyltetrahydrofurfurylalcohol (MTHFA), and also from the ring-opening of BHMTHF, such as 1,2,6-hexanetriol (1,2,6-HT) and tetrahydropyran-2-methanol (THPM), and from acetalization/etherification of HMF/BHMF, such as 5-(hydroxymethyl)furfural diethyl acetal (HMFDA), 5-(ethoxymethyl)furfuryl alcohol (EMFA), and 5-(ethoxymethyl)tetrahydrofurfuryl alcohol (EMTHFA) (Figures S1–S8), according to the reaction mechanism reported in Scheme S1. The lower selectivity ascertained in ethanol than in aqueous medium was related to the formation of a larger number of hydrogenolysis products together with compounds deriving from acetalization and etherification reactions, in addition to the compounds deriving from the opening-ring of BHMTHF already observed in water.[14]

In order to optimize the synthesis of BHMF and BHMTHF, the effect of the temperature decrease was investigated, and the obtained results are reported in Figure 1. The conversion of HMF (Figure 1A) was similar working at 100 and 80 °C, whilst it was strongly slowed down lowering the temperature to 50 °C, as evidenced by the HMF conversion of about 95 mol% reached only after 5 h. The BHMF yield (Figure 1B) reached a maximum, equal to about 62 mol% after 30 and 60 min at 100 and 80 °C, respectively, and then it decreased due to the conversion to BHMTHF, which reached a highest yield of about 89 mol% at both temperatures (Figure 1C). On the contrary, the trends of BHMF and BHMTHF yields were very different working at 50 °C. In fact, the BHMF yield increased during the whole investigated time, reaching the highest value of 58.8 mol% after 300 min together with the yield of BHMTHF of 25.8 mol% (Figure 1B,C). The values of carbon balance ascertained in the three runs are reported in Table S2 (runs 1–3), remaining almost constant in the whole investigated time range and similar (≈90 mol%) at the three temperatures. In conclusion, the results highlighted that temperatures higher than 50 °C were necessary to reach complete HMF conversion and promising diols yields. The influence of hydrogen pressure was investigated at 80 and 100 °C, and the obtained results are reported in Figure 2. The hydrogen pressure slightly influenced the HMF conversion at both 80 and 100 °C, and complete conversion was reached after 300 min under each investigated reaction condition (Figure 2A). On the other hand, the hydrogen pressure had a relevant influence on the products distribution; mainly, the decrease of pressure slowed down the hydrogenation of the furan ring of BHMF (Figure 2B,C). The highest BHMF yields ascertained at 60 and 50 bar were similar and equal to about 63 mol% working at both 100 and 80 °C, but they were reached at different time depending on the reaction conditions: working at 100 °C, the highest BHMF yield was reached after 15 min at 60 bar and after 30 min at 50 bar, whereas working at 80 °C, the highest BHMF yield was achieved after 30 min at 60 bar and after 60 min at 50 bar. Analogously, the highest BHMTHF yields were similar (≈90 mol%) working under the previous reaction conditions (60 and 50 bar; 100 and 80 °C), and they were reached working at 100 °C after 60 min at 60 bar and after 240 min at 50 bar, whereas working at 80 °C after 180 min at 60 bar and after 300 min at 50 bar. Noteworthy, the further decrease of pressure up to 20 bar allowed the marked slowdown of the hydrogenation of BHMF furan ring, thus increasing, as a consequence, the selectivity to this intermediate.

In fact, comparing, for example, the results at the same HMF conversion of about 93 mol% at 100 °C, the BHMF selectivity ascertained at 50 bar was lower than that obtained at 20 bar, being 57 and 86 mol%, respectively. As consequence, a significant improvement of BHMF yield was obtained and a yield of 80.2 mol% was ascertained after 60 min working at 100 °C.

At 20 bar, the decrease of temperature up to 80 °C allowed to reach the maximum BHMF yield at longer reaction time (180 min), together with a decrease to 74.2 mol%. Regarding the carbon balance (runs 1, 2, and 4–7, Table S2), as previously observed, it was almost constant (≈90 mol%) adopting temperatures of 100–80 °C at 50–60 bar. On the contrary, at 20 bar the carbon balance was low at short reaction time, increased with the prolonging of time, and decreased again for long reaction time. GC–MS analysis of the by-products evidenced that at short reaction times the concentration of HMFDA was higher at 20 bar than at the higher pressures (50 and 60 bar), indicating that at low hydrogen pressure the hydrogenation of HMF was slowed down and that other reaction pathways, such as its acetalization, were competitive. HMFDA was not quantified, and its higher amount contributed to the decrease of the carbon balance. However, as reported in the literature,[6b] the acetalization of HMF is an equilibrium reaction; thus, with the prolonging of time, the acetal can be re-converted to HMF, which can be hydrogenated to BHMF leading to the increase of

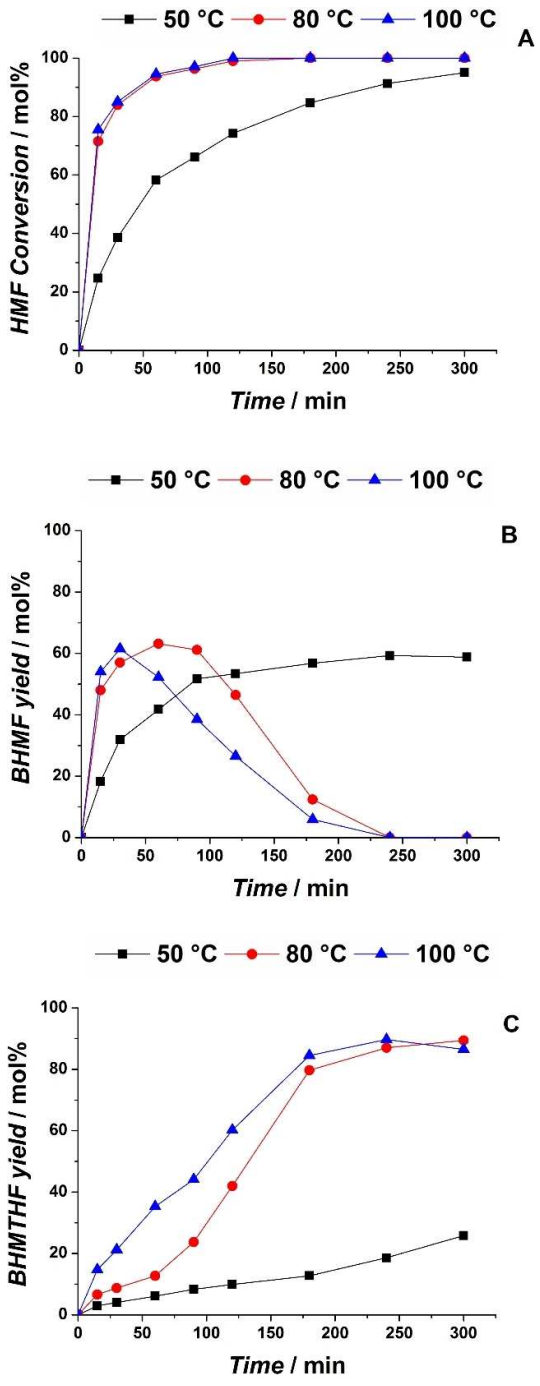

Figure 1. Influence of temperature on the HMF hydrogenation in the presence of 5 wt%Ru/C carried out with Ru/HMF ratio = 1 wt%, [HMF] = 3.7 wt%, 50 bar H_2, and 100 °C (run 1), 80 °C (run 2), and 50 °C (run 3).

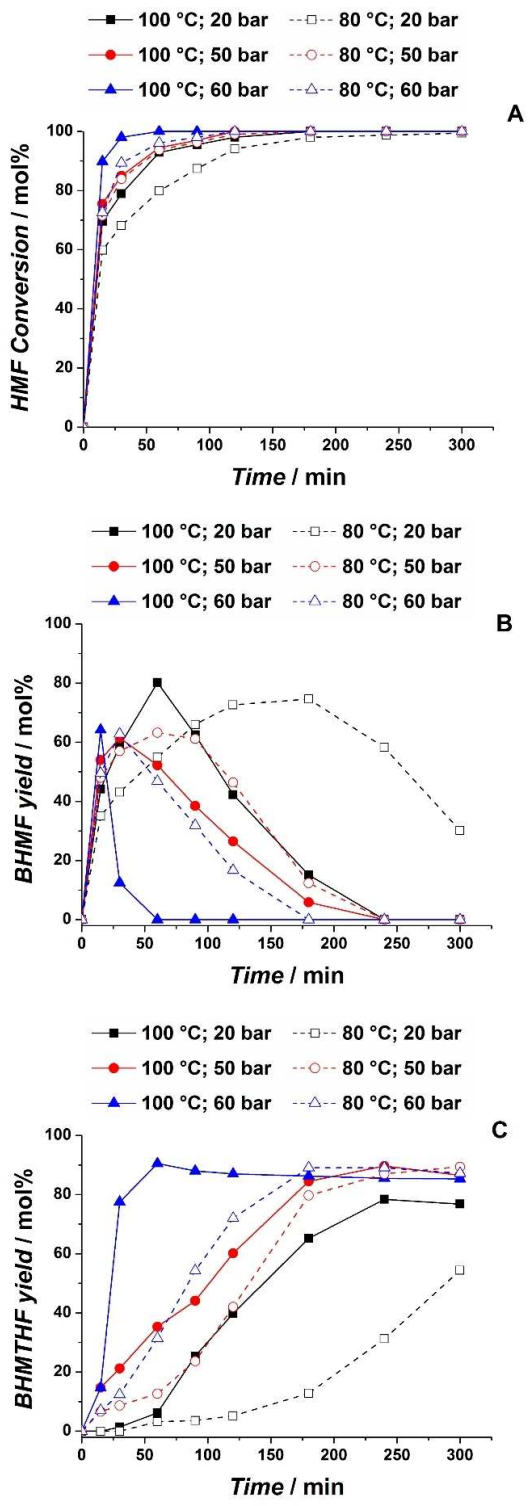

Figure 2. Influence of pressure on the HMF hydrogenation in the presence of 5 wt%Ru/C carried out with Ru/HMF ratio = 1 wt%, [HMF] = 3.7 wt% at 100 °C and 60 bar (run 4); 100 °C and 50 bar (run 1); 100 °C and 20 bar (run 5); 80 °C and 60 bar (run 6); 80 °C and 50 bar (run 2); 80 °C and 20 bar (run 7).

carbon balance. In addition, HMFDA, analogously to the acetal of furfural,[24] can be directly converted to EMFA, contributing to the formation of this by-product that originates also from the etherification of BHMF. In fact, at 20 bar the formation of EMFA was more significant than at 50 and 60 bar, since the etherification pathway at low hydrogen pressure is competitive with the hydrogenation of the furan ring of BHMF, thus causing the decrease of the carbon balance at long reaction time. As expected, the highest BHMF and BHMTHF yields were ascertained at the lowest (20 bar) and the highest (60 bar) investigated hydrogen pressure. Therefore, the pressure range was

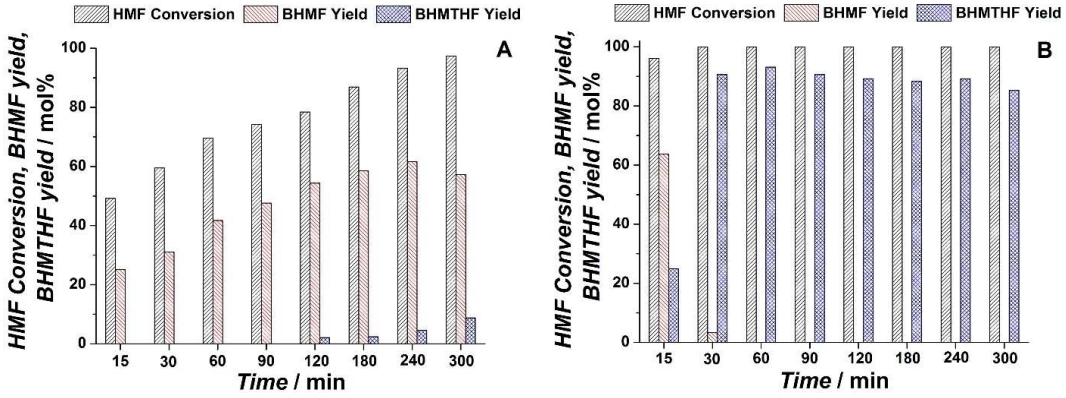

Figure 3. HMF hydrogenation in the presence of 5 wt%Ru/C carried out with Ru/HMF ratio = 1 wt%, [HMF] = 3.7 wt% at (A) 100 °C and 10 bar (run 8); (B) 100 °C and 70 bar (run 9).

further widened to 10–70 bar. The obtained results are reported in Figure 3.

The decrease of hydrogen pressure up to 10 bar caused a strong slowdown of the HMF conversion and the formation of BHMTHF was hampered, reaching after 300 min a yield lower than 10 mol% (Figure 3A). However, despite the marked reduction in BHMTHF formation, the yield of BHMF was not improved, with the highest ascertained BHMF yield and selectivity equal to 61.7 and 66.3 mol%, respectively, both lower than those reached working at 20 bar. This was due to the higher formation of by-products inherent the hydrogenation pathway, such as the HMFDA and EMFA at short and long reaction times, respectively, which caused the decrease of carbon balance since they were not quantified (run 8, Table S2). The obtained results highlight that an excessive decrease of hydrogen pressure limited the formation of BHMTHF but did not allow the optimization of BHMF yield because HMF and the target product were involved in other reactions. Therefore, the optimal reaction conditions for the synthesis of BHMF in ethanol were 100 °C, 20 bar, and 60 min. On the other hand, the increase of hydrogen pressure up to 70 bar allowed the selective formation of BHMTHF already at short reaction time (Figure 3B). The highest yield of 93.1 mol% was reached after 60 min and under these reaction conditions (100 °C and 70 bar), the trend of carbon balance was analogous to those ascertained working at 60 and 50 bar at the same temperature (run 9, Table S2). In conclusion, for the first time, the selective synthesis of each diol was performed in ethanol in the presence of the same commercial catalyst (5 wt%Ru/C).

In particular, the highest BHMF yield of about 80 mol% and the respective selectivity of 87 mol% were consistent with those already reported in the literature, but they were obtained at lower temperature, pressure, and reaction time, which are more sustainable reaction conditions (Table 1). Moreover, the highest BHMTHF yield of about 93 mol% was higher than that reported by Mishra et al.[18] and analogous to the value claimed by Bottari et al.,[16f] whilst the ascertained selectivity of 93 mol% was similar to those in the literature. Also, for BHMTHF, in this work its highest yield was ascertained working under more sustainable reaction conditions, adopting lower pressure and reaction time with respect to Mishra et al.[18] and lower temperature and reaction time with respect to Bottari et al.[16f] (Table 1). In addition, the employed catalyst 5 wt%Ru/C is cheaper than those reported in the literature (4 wt%Ru/$MnCo_2O_4$ and 5 wt% Pd/Al_2O_3), being a commercial catalyst and with Ru being cheaper than Pd.

Kinetic study of HMF hydrogenation

In order to investigate the kinetics of HMF hydrogenation, the presence of mass transfer phenomenon was assessed. On this basis, both internal and external limitations were investigated through the Weisz–Prater and the Mears criterions, respectively,[22,25] considering the reaction performed at 100 °C and 50 bar representative of the system. The Weisz–Prater and Mears parameters were equal to 0.005 and 4.02×10^{-7}, respectively (the numerical details regarding the calculation of both Weisz–Prater and Mears parameters are reported in the Supporting Information), from which it is possible to conclude that under the investigated reaction conditions the internal and external mass transfer were negligible. Once we had excluded the presence of mass transfer limitations, the kinetics of the HMF hydrogenation was investigated considering the following reactions (Scheme 2).

Due to the excess amount of H_2 with respect to HMF (molar ratio H_2/HMF = 34) and the constant presence of hydrogen pressure at 50 bar during the whole course of the reaction, which was guaranteed by the supply of hydrogen when necessary, the pseudo-first-order law model was adopted in order to calculate the kinetic rate constants and activation

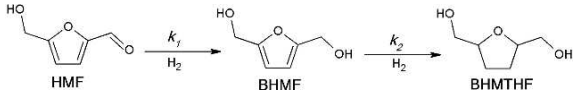

Scheme 2. Kinetics of the HMF hydrogenation.

energies of the reactions reported in Scheme 2. The differential Equations (1)–(3) were employed for this purpose:

$$\frac{d[HMF]}{dt} = -k_1[HMF] \quad (1)$$

$$\frac{d[BHMF]}{dt} = k_1[HMF] - k_2[BHMF] \quad (2)$$

$$\frac{d[BHMTHF]}{dt} = k_2[BHMF] \quad (3)$$

wherek_1 and k_2 are the pseudo-first-order rate constants of the reactions involved in the HMF hydrogenation at a selected temperature (in this case 100, 80, and 50 °C). By integration of the Equations (1)–(3) and considering the HMF concentration equal to the starting HMF concentration at the initial conditions of $t=0$ ($[HMF]_{t=0}=[HMF]_0$), the corresponding expressions relating the concentration of HMF, BHMF, and BHMTHF along time are expressed in the Equations (4)–(6), respectively:

$$[HMF] = [HMF]_0 \times e^{-k_1 t} \quad (4)$$

$$[BHMF] = [HMF]_0 \times \frac{k_1}{k_2 - k_1} \times (e^{-k_1 t} - e^{-k_2 t}) \quad (5)$$

$$[BHMTHF] = [HMF]_0 \times \frac{k_1}{k_2 - k_1} \times [e^{-k_2 t} + \frac{k_2}{k_1} \times (1 - e^{-k_1 t}) - 1] \quad (6)$$

Fitting the experimental data obtained at 100, 80, and 50 °C adopting Equations (4)–(6) and employing OriginPro software, it was possible to estimate the pseudo-first-order rate constants $k_1$and k_2. The activation energies of the reactions involved in the HMF hydrogenation were found from the Arrhenius law. The values of k_1 and k_2 obtained from the fitting at the three investigated temperatures are reported in Table 4, together with the activation energies derived from the graphs shown in Figure 4 that reports the Arrhenius plot.

Table 4. Calculated kinetic parameters for the hydrogenation of HMF.

T [K]	Rate constant [min^{-1}]		Activation energy [$kJmol^{-1}$]		R^2	
	k_1	k_2	k_1	k_2	k_1	k_2
323	0.0109	0.0021				
353	0.0523	0.0082	39.7	35.3	0.970	0.972
373	0.0685	0.0115				

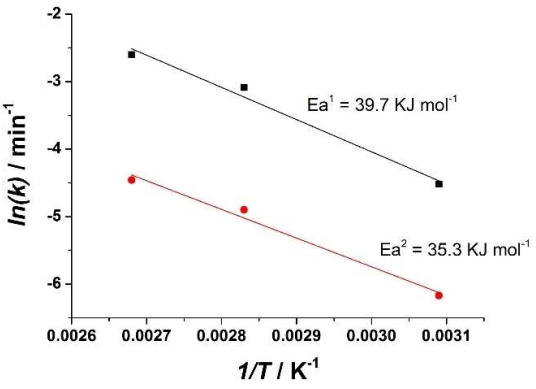

Figure 4. Arrhenius plot for the reactions involved in the HMF hydrogenation carried out at 50 bar.

Table 4 also reported the correlation coefficient R^2 that shows a good linearity at all the investigated temperatures, thus confirming the suitability of the pseudo-first-order reaction hypothesis for the hydrogenation of HMF.[26] The rate constant for the HMF hydrogenation to BHMF (k_1) is higher than that of the subsequent step (k_2), and the average ratio between k_1/k_2 is about 6 in the range of the investigated temperatures, proving that the hydrogenation of BHMF to BHMTHF is the rate-determining step, in agreement with the literature results.[27] This could be justified, as already reported in the literature, by the competitive adsorption of BHMF with HMF on the active sites of the catalyst and the stronger adsorption of HMF, which would hamper the hydrogenation of BHMF.[27] Due to this kinetic, the conversion of BHMF was slower than its formation, and thus it was not only possible to optimize the synthesis of the final product BHMTHF, but also that of the intermediate BHMF, by properly tuning the reaction conditions. Finally, it is possible to observe that at higher temperatures the rate constants increased, explaining the higher yields obtained working at elevated temperatures. On the other hand, the activation energies of the two reactions were similar, proving that the energy barriers of the two steps were almost analogous.

In addition, the order of reaction with respect to hydrogen pressure was investigated. For this purpose, the natural logarithms of reaction rates observed for the reactions performed at the same temperature (100 °C) and at different hydrogen pressure were plotted versus the natural logarithm of the respective pressure, as reported in Figure S10, which shows a linear dependence of reaction rate on hydrogen pressure; in particular, a first-order dependence between 10 and 70 bar was observed. This is in agreement with the literature results on the HMF hydrogenation, where the first-order dependence of reaction rate on hydrogen pressure has been already reported.[28]

Synthesis of BEMF

Once we had optimized the synthesis of BHMF and BHMTHF in ethanol, which represent not only interesting monomers for the synthesis of renewable resins, fibers, and foams,[29] we investigated their etherification to give new-generation biofuels, such as BEMF and BEMTHF, has been investigated. The etherification of pure BHMF with ethanol was studied in the presence of several commercial heterogeneous acid catalysts, such as sulfonated styrene–divenylbenzene resins (Amberlyst-15 and Amberlyst-70), perfluorosulfonic acid resin (Aquivion P87S), and, for the first time to the best of our knowledge, HZSM-5 zeolites having different Si/Al ratio (Si/Al = 15 and 25). The acid resins Amberlyst-15, Amberlyst-70, and Aquivion P87S are character-

ized by only Brønsted acid sites, and their total acidities are reported in the Experimental Section (Table 8). On the other hand, the zeolites are characterized by both Brønsted and Lewis acid sites, and thus a more deeply investigation of their acidic properties was performed by ammonia temperature-programmed desorption (NH_3-TPD) and diffuse reflectance infrared Fourier-transform spectroscopy (DRIFTS) of adsorbed pyridine. Regarding the NH_3-TPD analysis, the recorded profiles for the two zeolites are reported in Figure 5, together with the results in terms of ammonia desorption temperature and amount of desorbed ammonia, whereas in Table 5 the results are summarized.

The NH_3-TPD analyses of the fresh H-ZSM5 catalysts are in good agreement with the related literature and follow the expected trend of increasing acidity by decreasing the Si/Al ratio from 25 to 15.[30] In particular, the two characteristic peaks of ammonia desorption are observed, the first one centered at 262 °C and the second one between 470 and 500 °C, corresponding to weak and strong acid sites, respectively. A higher amount of weak acid sites was recorded for the zeolite HZSM-5 with Si/Al = 15 compared to that with Si/Al = 25, representing 66 and 54% of the total acidity, respectively, in agreement with the literature results.[31]

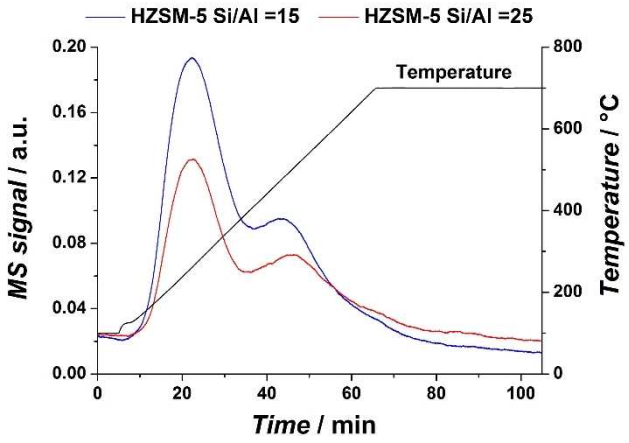

Figure 5. NH_3-TPD profiles of HZSM-5 (Si/Al = 15) and HZSM-5 (Si/Al = 25) in function of time. The corresponding heating ramp is reported on the secondary *y*-axis.

Table 5. NH_3-TPD results in terms of desorption temperature and amount of acid sites.

Sample	T_{max} desorption [°C]	NH_3 desorbed [mmol g^{-1}]	Overall NH_3 desorbed [mmol g^{-1}]
HZSM-5 (Si/Al = 25)	263 503	0.501 0.423	0.942
HZSM-5 (Si/Al = 15)	262 468	0.980 0.500	1.480

Regarding the DRIFTS of pyridine performed on the zeolites HZSM-5 with Si/Al = 15 and 25, the spectra recorded in function of the increasing temperature of the sample are shown in Figure S11. All investigated samples showed bands at around 1640, 1491, and 1541 cm^{-1}, characteristic of pyridinium ions (Brønsted acid sites), and bands at around 1600, 1575, and 1444 cm^{-1}, characteristic of coordinatively bound pyridine over Lewis acid sites. In both samples, during the desorption, a faster decrease of the intensity of bands associated to Lewis acid sites is observed, demonstrating a stronger adsorption of pyridine over Brønsted sites, pointing out that the Brønsted sites are stronger than the Lewis ones in both samples.

These catalysts were tested under the same reaction conditions (60 °C, 4 h; $mol_{BHMF}/mol_{total\ acid\ sites}$ = 8.3; [BHMF] = 3 wt %) and adopting equal amount of introduced total acid sites, with the aim to identify the most promising one. The starting BHMF concentration was the value reached in its above-described optimized synthesis, in the perspective of implementing a possible cascade process. The obtained results are reported in Table 6. Except for the zeolite HZSM-5 with Si/Al = 15, all the other catalysts gave a complete BHMF conversion, showing that the formation of the mono-ether EMFA was fast, while the kinetic limiting step was the etherification of the second hydroxy group, as already reported in the literature.[6b] The high activity of acid resins was due to the presence of only Brønsted acid sites that strongly promoted the conversion of BHMF. However, adopting acid resins, lower selectivities towards the etherification products and lower carbon balance values were obtained than those ascertained with zeolites, which have both Brønsted and Lewis acid sites (Table 6). In particular, employing the zeolite HZSM-5 (Si/Al = 25), a BEMF selectivity of 63.3 mol% was obtained at complete BHMF conversion, which was almost double of the BEMF selectivities ascertained with the acid resins. In fact, it is well known that the Brønsted acidity promotes the formation of by-products, such as 2,5-dihydro-2-ethoxy-2-(ethoxymethyl)-5-methylenefuran (DHEMMF, Figure S12) and 1-ethoxy-3-hexene-2,5-dione (EHED, Figure S13), deriving, respectively, from the hydration of BHMF and the successive opening-ring, as reported in Scheme S2.[20a,32–34]

Table 6. Comparison of different commercial heterogeneous acid catalysts in the etherification of BHMF with ethanol under the same reaction conditions.[a]

Run	Catalyst	BHMF conv. [mol%]	EMFA yield [mol%]	BEMF yield [mol%]	Carbon balance[b] [mol%]
ETER_1	Amberlyst-15	100	18.5	37.5	56.0
ETER_2	Amberlyst-70	100	14.7	32.4	47.1
ETER_3	Aquivion P87S	100	18.9	25.6	44.5
ETER_4	HZSM-5 (Si/Al = 25)	100	16.4	63.3	79.7
ETER_5	HZSM-5 (Si/Al = 15)	50.7	39.1	5.5	93.9

[a] $mol_{BHMF}/mol_{total\ acid\ sites}$ = 8.3; [BHMF] = 3.0 wt%; T = 60 °C; t = 4 h. [b] Carbon balance = $[(mol_{unconvertedBHMF} + mol_{EMFA} + mol_{BEMF})/mol_{startingBHMF}] \times 100$

On the other hand, the lower activity of the zeolite HZSM-5 (Si/Al = 15), also with respect to the zeolite HZSM-5 (Si/Al = 25), cannot be related to the surface area because the two zeolites have quite similar surface areas (442 and 401 $m^2 g^{-1}$, respectively), but it should be related to the lower percentage of strong acid sites, as evidenced by the NH_3-TPD analysis (Figure 5). Therefore, working with the same number of total acid sites, a larger amount of strong acid sites has been introduced employing the zeolite with Si/Al = 25, which allowed the complete BHMF conversion and the higher yield of BEMF (compare runs ETER_4 and ETER_5, Table 6). Due to the more promising performances afforded by the zeolites HZSM-5, they have been further studied to verify the influence of reaction time and temperature on the etherification. The obtained results working at 60 and 80 °C in a time range between 2 and 8 h are reported in Figure 6.

Working at 60 °C in the presence of the zeolite HZSM-5 with Si/Al = 15, the prolonging of reaction time allowed the increase of BHMF conversion up to 78.2 mol% after 8 h (Figure 6A). Moreover, the yield of BEMF was slightly improved, but it was only 10.5 mol% after 8 h, showing that the kinetics was very slow under this reaction condition, and the major product was still EMFA after long time, with the yield of 49.0 mol%. However, the increase of temperature up to 80 °C strongly sped up the reaction, allowing the complete BHMF conversion after 4 h and the improvement of BEMF yield up to 40.4 mol% after 8 h, although the EMFA yield was still 31.0 mol% after the same time. On the other hand, the zeolite HZSM-5 with Si/Al = 25 led to complete BHMF conversion already after 2 h working at 60 °C and at this temperature the prolonging of reaction time allowed the etherification of EMFA to BEMF to reach the yield of 69.7 mol% after 8 h, confirming the higher activity of this catalyst. Also in this case, the increase of temperature up to 80 °C strongly sped up the formation of BEMF, which after only 2 h reached the yield of 73.6 mol%. However, under these reaction conditions the prolonging of reaction time did not improve the formation of BEMF, and at longer time its yield slightly decreased to 64.6 mol% due to the formation of by-products. As shown in Figure 6D, although the increase of temperature promoted the BEMF synthesis, it also caused the decrease of carbon balance for both zeolites due to the higher formation of by-products. Finally, comparing the carbon balance values obtained with the two zeolites, it is evident that the zeolite with Si/Al = 15 led to lower amount of by-products than Si/Al = 25 at both investigated temperatures, probably due to the lower percentage of strong acid sites. However, higher BEMF yields and selectivities were ascertained in the presence of the zeolite HZSM-5 with Si/Al = 25, which was the best catalyst leading to BEMF yield of 73.6 mol% working at 80 °C after 2 h. The ascertained BEMF yield is analogous to the majority of the values already reported in the literature, but it was obtained after shorter reaction time because generally times longer than 8 h have been adopted (Table 2).

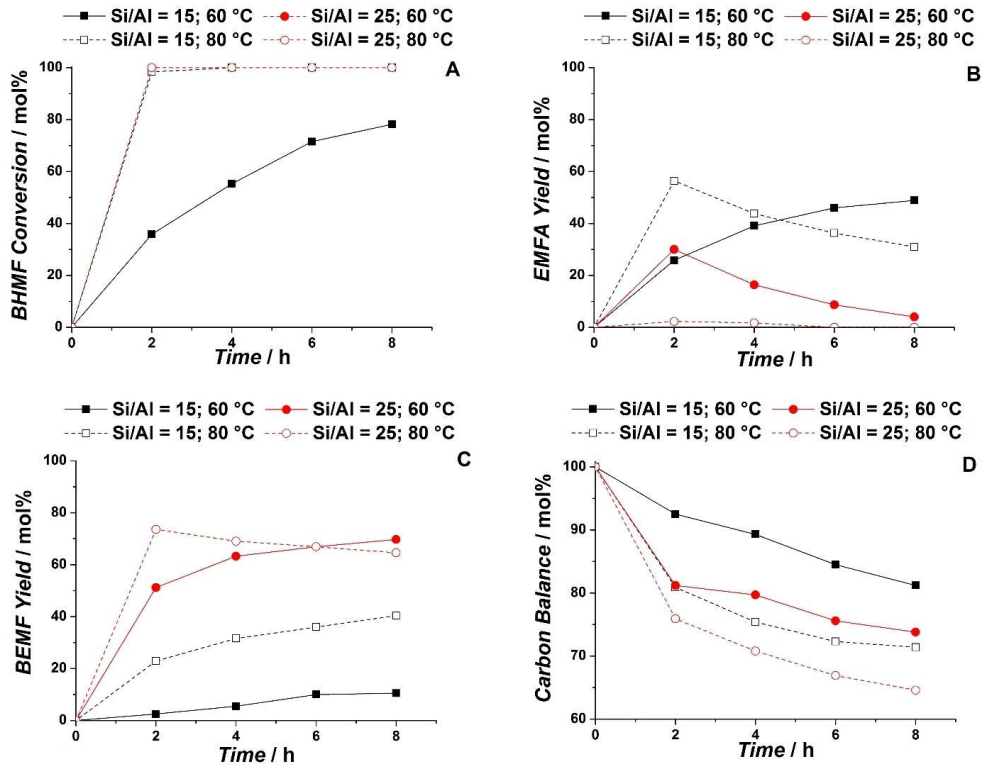

Figure 6. Pure BHMF etherification carried out with the two zeolites HZSM-5 having Si/Al = 15 and Si/Al = 25 adopting $mol_{BHMF}/mol_{total\ acid\ sites} = 8.3$, [BHMF] = 3.0 wt% at 60 and 80 °C. Note: in Figure 6A the curves of BHMF conversion at 60 and 80 °C with zeolite HZSM-5 having Si/Al = 25 and that of BHMF conversion at 80 °C with zeolite HZSM-5 having Si/Al = 15 are overlapped.

The optimized reaction conditions were adopted for the etherification of crude BHMF deriving from the optimized hydrogenation of HMF. In this case only a slight decrease of BEMF yield and selectivity was observed, at 71.2 mol% instead of 73.6 mol% as previously ascertained starting from pure BHMF. The obtained results are very promising because they show that the reaction conditions optimized for the etherification of pure BHMF are valid also for a sustainable cascade process from the hydrogenation reaction mixture. Moreover, the reached BEMF yield is in line with those already reported in the literature, as in the work of Han et al., who etherified the crude BHMF in the presence of Amberlyst-15 as catalyst at 60 °C for 10 h claiming a BEMF yield of 70 mol%.[19b] On the other hand, Balakrishnan et al. carried out the one-pot conversion of HMF to BEMF at 60 °C for 18 h employing a hydrogenation catalyst (5 wt%Pt/Al_2O_3) and an acid catalyst (Amberlyst-15) with a hydrogen pressure of 14 bar reaching the BEMF yield of 59 mol% with respect to the starting HMF,[15a] a value analogous to the BEMF yield achieved in our cascade process calculated with respect to the starting HMF (57 mol%). Although the obtained BEMF yield is similar to those already reported in the literature, it is noteworthy to underline that much shorter reaction time was necessary in the present work.

Synthesis of BEMTHF

Analogously to the etherification of BHMF, the etherification of BHMTHF was also studied. However, as already found in the literature for the etherification of tetrahydrofurfuryl alcohol,[35,36] independently of the employed catalyst and the adopted reaction conditions, BEMTHF was not obtained. This could be due to the absence of unsaturated bonds in the chemical structure of BHMTHF that gives low reactivity at the hydroxy groups. On the other hand, BHMF, similarly to the benzyl structure, has an aromatic character due to the furan ring; thus, the hydroxy groups have higher reactivity, and as consequence it can be easily etherified, as previously observed.[35] For this reason, it was not possible to synthesize BEMTHF through the direct etherification of BHMTHF, while the hydrogenation of the furan ring of BEMF can represent a feasible way. In order to explore this route, BEMF obtained from the etherification of the crude BHMF was hydrogenated in the presence of the same 5 wt%Ru/C as catalyst previously adopted also for the hydrogenation of HMF to diols. Moreover, 5 wt%Ru/C was already employed in the hydrogenation of furan ethers, such as in the hydrogenation of ethyl furfuryl ether to ethyl tetrahydrofurfuryl ether.[35] To the best of our knowledge, this is the first time that the hydrogenation of BEMF to BEMTHF has been investigated. On the basis of the previous adopted reaction conditions for the reduction of the furan ring, a preliminary study of the hydrogenation of BEMF has been carried out, investigating the influence of temperature and hydrogen pressure. The obtained results are reported in Figure 7. The adopted reaction conditions allowed the reduction of the furan ring of BEMF, leading to the formation of the desired product BEMTHF (Figures S14 and S15), reaching the yield of 40.2 mol% after 300 min at

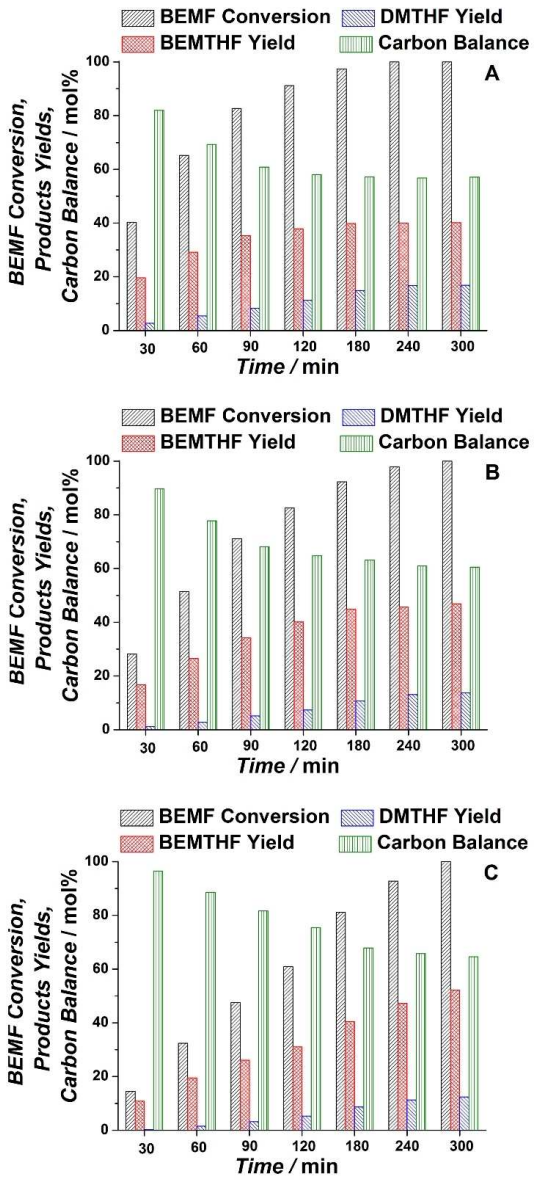

Figure 7. Crude BEMF hydrogenation carried out with commercial 5 wt%Ru/C adopting the Ru/BEMF ratio = 0.8 wt% at (A) 100 °C and 60 bar; (B) 80 °C and 60 bar; (C) 80 °C and 40 bar.

100 °C and 60 bar (Figure 7A). However, already after 30 min the amount of by-products was not negligible. In particular, by-products deriving from hydrogenolysis were identified, such as the 2,5-dimethyltetrahydrofuran (DMTHF) (Figure S16), whose amount increased with the prolonging of time, analogously to the other by-products, up to the yield of about 16.9 mol% after 300 min. In fact, a recent work found that the C–O bond cleavage of 2,5-bis(alkoxymethyl)furans is easier and faster than the respective diols; thus, the hydrogenolysis was promoted in this reaction.[37] In order to investigate the role of temperature and promote the hydrogenation respect to the hydrogenolysis, the temperature was decreased to 80 °C, keeping the pressure at 60 bar (Figure 7B). Under these second reaction conditions, the conversion of BEMF was slowed down and the formation of

DMTHF was partially limited, finally reaching a yield of 13.7 mol% after 300 min together with a BEMTHF yield of 46.9 mol%, a value higher than that previously obtained, proving that the decrease of temperature promoted the BEMTHF synthesis. Moreover, the formation of the other by-products was also slightly limited, as evidenced by the higher values of carbon balance obtained at 80 °C. The decrease of temperature from 100 to 80 °C improved the BEMTHF selectivity from 40.2 to 46.9 mol% at complete BEMF conversion. Finally, the influence of the hydrogen pressure was investigated by decreasing it to 40 bar and keeping the temperature at 80 °C (Figure 7C). Under these reaction conditions, the conversion of BEMF was further slowed down, but the lower pressure did not hamper the DMTHF formation, whose yield after 300 min was 12.4 mol%, similar to that obtained at 60 bar. However, the yield of BEMTHF was slightly improved to 52.2 mol% thanks to the reduction of the amount of the other by-products. In fact, with the decrease of pressure from 60 to 40 bar the carbon balance after 300 min was improved from 60.6 to 64.6 mol%.

In conclusion, 80 °C and 40 bar allowed the highest BEMTHF yield of 52.2 mol%. However, due to the relevance of this new product, a deeper investigation of the reaction and, above all, a fine-tuning of the catalytic system appear necessary for the optimization of this unexplored route, and some studies are now in progress.

Catalyst recyclability

The stability and recyclability of the adopted heterogeneous catalysts is a fundamental issue in order to propose a robust process. Thus, recyclability tests were performed for both the catalysts employed in the hydrogenation of HMF and in the etherification of BHMF. Regarding the first one, 5 wt%Ru/C recovered from the optimized synthesis of BHMF (100 °C, 20 bar, and 60 min) was reused in four subsequent runs under the same reaction conditions, and the obtained results are reported in Figure S17A. During the five hydrogenation cycles, only a slight decrease of catalytic activity was observed, which in particular took place after the fourth cycle (Figure S17A). In fact, the HMF conversion decreased by about 11.8 mol% and as consequence also a decrease of BHMF and BHMTHF yields was ascertained. However, the carbon balance was almost constant in the five cycles decreasing by only about 2 mol% from 1st to 5th cycle, thus showing that only the catalytic activity decreased but the selectivity of the reaction was almost unchanged. The slight loss of catalytic activity is due to the carbon deposition on the catalyst surface, as shown by the thermogravimetric analysis (TGA; Figure S18). This is also confirmed by higher mass loss recorded for the recycled catalyst than for the fresh one, as shown in Table 7, together with other textural properties of fresh and spent 5 wt%Ru/C. The high mass loss highlights that organic matter was present, causing the passivation of the catalyst surface, as confirmed by the lower surface area of the employed catalyst with respect to the fresh one (576 and 770 $m^2 g^{-1}$, respectively). In particular, the blockage of micropores due to humins deposition can be observed by the changes of the textural properties of the fresh and recycled catalysts. In fact, the micropore area and the micropore volume represented 53 and 43% of the total area and total volume in the fresh catalyst, respectively, whereas these values decreased to 36 and 22%, respectively, in the recycled catalyst (Table 7). It is well-known that during the HMF hydrogenation also the polymerization mechanism takes place, leading to the formation of humins, which generally represents the main reason of catalyst deactivation.[14,16b,d,22] Regarding the recyclability of the catalyst employed in the etherification of BHMF, the zeolite HZSM-5 with Si/Al = 25 recovered from the optimized synthesis of BEMF (80 °C, 2 h) was reused in four subsequent runs under the same reaction conditions, and the obtained results are reported in Figure S17B, whilst the textural properties of the fresh catalyst and spent one recovered at the end of the fifth cycle are shown in Table 7. Complete conversion of BHMF was reached in each recycle test, even if the BEMF yield decreased from 73.6 to 60.1 mol%, together with the increase of EMFA yield from 2.3 to 13.0 mol% after five cycles, thus confirming that the etherification of the first hydroxy group of BHMF is very fast with the zeolite HZSM-5 (Si/Al = 25). On the other hand, the etherification of EMFA to BEMF was slightly limited. In this case, too, the slight loss of activity was due to the carbonaceous material deposition on the catalyst surface, as shown by TGA that evidenced a slightly higher weight loss for the catalyst after five cycles than the fresh one (Figure S19). The textural properties reported in Table 7 highlight the decrease of the catalyst surface area after five cycles, from 401 to 313 $m^2 g^{-1}$ for the fresh and spent ones, and in particular the blockage of micropores due to the humins deposition. In fact, the micropore area and the micropore

Table 7. Textural properties and weight loss of fresh and spent catalysts adopted in the hydrogenation of HMF (5 wt%Ru/C) and in the etherification of BHMF (zeolite HZSM-5 Si/Al = 25), yields of the respective products (BHMF and BEMF), and carbon balance obtained in the first and fifth cycles after the same time of 60 min.

Properties	5 wt%Ru/C				Zeolite HZSM-5 (Si/Al = 25)			
	Fresh		Recovered after 5th cycle		Fresh		Recovered after 5th cycle	
Specific surface area [$m^2 g^{-1}$]	770		576		401		313	
Micropore area [$m^2 g^{-1}$]	413		209		281		196	
Total pore volume [$cm^3 g^{-1}$]	0.46		0.32		0.54		0.47	
Micropore volume [$cm^3 g^{-1}$]	0.20		0.07		0.10		0.04	
Weight loss [%]	20.5		34.3		1.8		3.0	
Yield after 60 min [mol%]	80.2 (BHMF)	6.2 (BHMTHF)	69.5 (BHMF)	3.2 (BHMTHF)	73.6 (BEMF)	2.3 (EMFA)	60.1 (BEMF)	13.0 (EMFA)
Carbon balance after 60 min [mol%]	93.5		91.6		75.9		73.1	

volume represented 70 and 19% of the total area and total volume in the fresh catalyst, respectively, whereas these values decreased to 63 and 9%, respectively, in the recycled catalyst (Table 7). However, these changes are less relevant than those reported for the catalyst employed in the HMF hydrogenation, probably due to the lower formation of heavy by-products during the etherification step, in agreement with TGA. The lower amount of heavy by-products formed during the etherification seems in disagreement with the carbon balance results, which were lower for the etherification reaction, but this can be justified considering the non-negligible formation of other not quantified soluble by-products, such as DHEMMF and EHED, which apparently were the main by-products of this reaction. However, both 5 wt%Ru/C and HZSM-5 (Si/Al = 25) showed only a slight decrease of activity after five cycles, indicating stability and recyclability. In addition, as already reported in the literature, they could be easily reactivated through washing with acetone and calcination procedures, respectively.[14,17,22,39]

Conclusion

The proposed cascade process represents a novel strategy for the valorization of the platform chemical 5-hydroxymethylfurfural (HMF) to the diol monomers 2,5-bis(hydroxymethyl)furan (BHMF) and 2,5-bis(hydroxymethyl)tetrahydrofuran (BHMTHF), which are promising monomers, and to the two furan ethers 2,5-bis(ethoxymethyl)furan (BEMF) and 2,5-bis(ethoxymethyl)tetrahydrofuran (BEMTHF), which can represent promising biofuels. In the first step, the hydrogenation of HMF to diols was investigated in ethanol employing a commercial 5 wt%Ru/C as catalyst. For the first time, each diol was selectively obtained in ethanol in the presence of the same catalyst by simply tuning the reaction conditions, reaching the highest yield of about 80 and 93 mol% of BHMF and BHMTHF, respectively. In the second step, the etherification of both pure BHMF and BHMTHF to give BEMF and BEMTHF, respectively, was studied by testing several commercial acid heterogeneous catalysts and different reaction conditions. The zeolite HZSM-5 with Si/Al ratio of 25 was the most promising catalyst in the etherification of BHMF, leading to the highest activity and selectivity towards the desired product BEMF. Analogous results were also achieved starting from crude BHMF, scarcely studied in the literature, showing the feasibility of the cascade process for the synthesis of BEMF from HMF. On the contrary, BEMTHF was not obtained by the direct etherification of BHMTHF, independently of the employed catalyst and the adopted reaction conditions, due to the low reactivity of its hydroxy groups. A preliminary investigation evidenced the possibility of obtaining BEMTHF by adopting, for the first time, a novel route via hydrogenation of BEMF in the presence of commercial 5 wt%Ru/C as catalyst. The above proposed cascade approaches involving hydrogenation and etherification open the way to the selective production of both important monomers, BHMF and BHMTHF, and of the respective ether biofuels, BEMF and BEMTHF, in the presence of stable and recyclable catalysts.

Experimental Section

Materials

5-Hydroxymethylfurfural (95%) was supplied by AVA Biochem. 2,5-Bis(hydroxymethyl)furan (95%) and 2,5-bis(hydroxymethyl)tetrahydrofuran (95%) were provided by AKos GmbH. 5 wt%Ru/C, ethanol (96%), toluene (> 99%), and 2,5-dimethyltetrahydrofuran (96%) were purchased from Sigma-Aldrich. Amberlyst-70 and Amberlyst-15 were provided by Rohm and Haas. Aquivion P87S was obtained by Solvay Specialty Polymers. Two commercial zeolites HZSM-5 having Si/Al equal to 15 and 25 (Zeocat PZ-2/25H and Zeocat PZ-2/50H) were purchased from ZeoChem AG. The catalysts were dried at 90 °C under reduced pressure for 3 h before their employment. Since all the employed acid catalysts are commercial, their characteristics are reported in the literature and summarized in Table 8.

Hydrogenation of HMF

Hydrogenation reactions were conducted in a 300 mLstainless-steel Parr 4560 autoclave equipped with a P.I.D. controller (4843). The catalyst, employed as received, was weighed (0.3 g, corresponding to a metal/HMF weight ratio of 1 wt%) and introduced into the autoclave, which was then closed, flushed with nitrogen, and evacuated to 65 Pa with a mechanical vacuum pump in order to introduce by suction 50 mL of an HMF/ethanol solution (30 g L^{-1}, corresponding to a substrate loading of 3.7 wt%). Subsequently, the reactor was pressurized with 3 bar of hydrogen and heated to the defined temperature, and the reaction mixture was stirred using a mechanical overhead stirrer. When the temperature reached the established value, pressure was raised to the desired value and the reaction time started. The pressure in the reactor was kept constant by hydrogen addition, when necessary. The reaction was monitored by sampling periodically the liquid through a dip tube and the collected liquid samples were analyzed through GC–FID (flame ionization detector) and GC–MS. For the recycling tests, the spent catalyst was recovered through filtration, washed with ethanol, dried under vacuum at 40 °C overnight, and used for the subsequent run. This procedure was repeated four times.

Etherification of pure diols

The etherification of pure BHMF and BHMTHF was carried out in a 60 mL glass reactor, and their starting concentrations were equal to those ascertained in the respective optimized synthesis, in order to reproduce the cascade process. The substrate, ethanol, and the acid heterogeneous catalyst were weighed and filled into the reactor, then it was closed and put in an oil bath, previously heated to the desired temperature, and the mixture was kept under magnetic stirring. At the end of the run, the reactor was rapidly cooled under cool air flow, and the catalyst was separated from the reaction mixture through centrifugation. The liquid fraction was analyzed through GC–FID and GC–MS. For the recycling tests, the recovered

Table 8. Acidity of the commercial catalysts employed in the etherification.

Catalyst	Total acidity[a] [mmol g^{-1}]	Ref.
Amberlyst-15	4.70	[40]
Amberlyst-70	2.55	[40]
Aquivion P87S	1.15	[40]

[a] Evaluated by NaOH titration in 2 M solutions of NaCl

catalyst was washed with ethanol, dried under vacuum at 40 °C overnight, and used for the subsequent run. This procedure was repeated four times.

Etherification of crude BHMF

The etherification of crude BHMF obtained from its optimized synthesis was carried out as reported above for pure BHMF, and the liquid fraction was analyzed through GC–FID and GC–MS.

Hydrogenation of crude BEMF

The hydrogenation of crude BEMF obtained from the etherification of crude BHMF was carried out using the same autoclave employed for the hydrogenation of HMF, and an analogous experimental procedure was adopted. The reaction was monitored by periodically sampling the liquid reaction mixture through a dip tube and analyzing it through GC–FID and GC–MS.

Product analysis

The liquid samples were analyzed using GC–FID (Perkin Elmer Clarus series GC) equipped with a SUPELCOWAX-10 column (30 m × 0.53 mm × 1.0 μm). Nitrogen was employed as the carrier gas with flow of 1 mL min^{-1}. The injector was kept at 250 °C, the detector was maintained at 280 °C, and the following temperature program was adopted for the chromatographic run: 40 °C isothermal for 2 min; 20 °C min^{-1} up to 160 °C; 160 °C isothermal for 2 min; 10 °C min^{-1} up to 250 °C; 250 °C isothermal for 5 min. The concentrations of HMF, BHMF, and BHMTHF in the mixtures collected from the HMF hydrogenation were calculated on the base of standard calibration curves previously prepared by injecting standard solutions. The FID response factors of EMFA, BEMF, and BEMTHF were estimated by the effective carbon number (ECN) method, which is a recognized alternative way to predict FID response.[41] The experiments were carried out in triplicate, and the reproducibility of the techniques was within 3 %.

The identification of the component present in the reaction mixture was performed by gas chromatography coupled with mass spectrometer (GC–MS). A GC-MS (Agilent 7890B-5977 A) equipped with HP-5MS capillary column (30 m × 0.25 mm × 0.25 μm) (5 %-phenyl)-methylpolysiloxane was used for the analysis. The carrier gas was helium with a flow of 1 mL min^{-1}. The injector and detector temperatures were 250 and 280 °C, respectively, and the following temperature program was adopted for the chromatographic run: 70 °C isothermal for 3 min; 5 °C min^{-1} up to 110 °C; 2 °C min^{-1} up to 130 °C; 20 °C min^{-1} up to 250 °C; 250 °C isothermal for 1 min. The identification of the compounds was done by comparing their spectra with those present in the Wiley Registry 10th Edition.

Catalyst characterization

The total acidity of zeolites was measured by NH_3-TPD using a MicromeriticsAutoChem II 2920 instrument. A suitable trap of soda lime was used to block any moisture desorption while effluents were analyzed using a thermal conductivity detector (TCD). Typically, 0.15 g of sample was charged in a quartz tube and heated up to 450 °C in a 5 % of O_2 in He flow (30 mL min^{-1}) with a heating rate of 15 °C min^{-1}. The final temperature was kept for 60 min to clean the catalyst surface. After cooling, NH_3 chemisorption was performed at 100 °C by flowing a 30 mL min^{-1} of 10 % NH_3/He for 30 min. Before desorption, samples were flowed with He (30 mL min^{-1}) for 40 min at the adsorption temperature to remove the weakly physisorbed ammonia. Lastly, TPD was performed under the same He flow with a heating rate of 10 °C min^{-1} to 700 °C, temperature kept for 40 min.

In-situ DRIFTS of adsorbed pyridine, followed by desorption at increasing temperature, was carried out with a Bruker Vertex 70 instrument equipped with a Pike DiffusIR cell attachment and an MCT (Mercury-Cadmium-Telluride) detector to characterize the distribution of Lewis and Brønsted acidic sites in HZSM-5 catalysts. Spectra were recorded carrying out 128 scans in the spectral region of 4000–600 cm^{-1} with a resolution of 4 cm^{-1}. The spectra were recorded as follows: first, KBr was loaded in the DRIFTS cell and pre-treated at 500 °C under a flow of He (10 mL min^{-1}) for 30 min in order to remove adsorbed molecules. Then, the cell was cooled down to 50 °C, and the background spectra were acquired at different temperatures (with steps of 50 °C up to 500 °C). Then, HZSM-5 was loaded in the DRIFTS cell and was subjected to the same procedure: a pre-treatment at 500 °C in He flow for 60 min, cooling to 50 °C, and recording of spectra every 50 °C until 500 °C. Next, the adsorption of pyridine was carried out after cooling down to 50 °C by injecting a pulse (2 μL) in the He flow (pre-heated at 150 °C). The adsorption process was monitored by recording a spectrum every minute until the intensity of the bands of pyridine in the spectra remained constant. Finally, spectra of adsorbed pyridine over the catalyst were recorded every 50 °C, increasing the temperatures up to 500 °C.

Nitrogen adsorption/desorption isotherms (77 K) were recorded using a Micromeritics ASAP 2020 instrument. Samples were previously outgassed for 120 min at 423 K and 30 μm Hg and then heated for 240 min at 623 K. Specific surface area values were obtained using the multi-point Brunauer–Emmett–Teller (BET) equation in the 0.05–0.2 p/p_0 range and total pore volume values were calculated at 0.95 p/p_0.

TGA was performed with a Mattler Toledo TGA/SDTA 851 apparatus using a temperature ramp from 20 to 650 °C with a heating rate of 10 °C min^{-1} under nitrogen atmosphere for the fresh and spent 5 wt%Ru/C and under air atmosphere for the fresh and spent zeolite HZSM-5 (Si/Al = 25).

Acknowledgements

Marco Martinelli and AntonellaManariti of the Department of Chemistry and Industrial Chemistry of the University of Pisa are gratefully acknowledged for their precious technical support. Open Access Funding provided by Universita degli Studi di Pisa within the CRUI-CARE Agreement.

Conflict of Interest

The authors declare no conflict of interest.

Data Availability Statement

The datathatsupportthefindingsofthisstudyareavailable in the-supplementary material ofthisarticle.

Keywords: 5-hydroxymethylfurfural · furan ether · heterogeneous catalysis · hydrogenation · tetrahydrofuran ether

[1] S. Puricelli, G. Cardellini, S. Casadei, D. Faedo, A. E. M. van den Oever, M. Grosso, *Renewable Sustainable Energy Rev.* **2021**, *137*, 110398–110416.
[2] a) P. Mäki-Arvela, D. Ruiz, D. Y. Murzin, *ChemSusChem* **2021**, *14*, 150–168; b) N. Ayoub, J. Toufaily, E. Guénin, G. Enderlin, *ChemSusChem* **2022**, e202102606; c) Y. He, L. Deng, Y. Lee, K. Li, J. M. Lee, *ChemSusChem* **2022**, e202200232; d) Y. Meng, S. Yang, H. Li, *ChemSusChem* **2022**, e202102581.
[3] C. Rosenfeld, J. Konnerth, W. Sailer-Kronlachner, T. Rosenau, A. Potthast, P. Solt, H. W. G. van Herwijnen, *ChemSusChem* **2020**, *13*, 5408–5422.
[4] X. Yue, Y. Queneau, *ChemSusChem* **2022**, e202102660.
[5] a) X. P. Nguyen, A. T. Hoang, A. I. Ölçer, D. Engel, V. V. Pham, S. K. Nayak, *Fuel Process. Technol.* **2021**, *214*, 106687–106722;b) L. Hu, Y. Jiang, X. Wang, A. He, J. Xu, Z. Wu, *Biomass Convers.Biorefin.* **2020**, 1–16; c) Y. Wan, J. M. Lee, *ChemSusChem* **2021**, *14*, 1–26; d) J. E. Rorrer, A. T. Bell, F. D. Toste, *ChemSusChem* **2019**, *12*, 2835–2858.
[6] a) E. De Jong, G. Gruter, *SAE Technical paper* 2009–01-2767 **2009**, Doi:10.4271/2009-01–2767; b) E. R. Sacia, M. Balakrishanan, A–T. Bell, *J. Catal.* **2014**, *313*, 70–79; c) F. Zaccheria, N. Scotti, N. Ravasio, *Catalysts* **2019**, *9*, 172–192.
[7] a) S. Alipour, H. Omidvarborna, D.-S. Kim, *Renewable Sustainable Energy Rev.* **2017**, *71*, 908–926; b) J. Wei, T. Wang, H. Liu, M. Li, X. Tang, Y. Sun, X. Zeng, L. Hu, T. Lei, L. Lin, *Energy Technol.* **2019**, *7*, 1801071–1801081.
[8] a) K. Barbera, P. Lanzafame, A. Pistone, S. Millesi, G. Malandrino, A. Gulino, S. Perathoner, G. Centi, *J. Catal.* **2015**, *323*, 19–32; b) P. Lanzafame, G. Papanikolaou, S. Perathoner, G. Centi, M. Migliori, E. Catizzone, G. Giordano, *Appl. Catal. A* **2019**, *580*, 186–196; c) P. Lanzafame, G. Papanikolaou, K. Barbera, G. Centi, S. Perathoner, *J. Energy Chem.* **2019**, *36*, 114–121.
[9] a) G. J. M.Gruter, WO2009/030509A2, Furanix Technologies B.V. (2009); b) F. Zaccheria, F. Bossola, N. Scotti, C. Evangelisti, V. Dal Santo, N. Ravasio, *Catal. Sci. Technol.* **2020**, *10*, 7502–7511.
[10] a) Q. Cao, W. Liang, J. Guan, L. Wang, Q. Qu, X. Zhang, X. Wang, X. Mu, *Appl. Catal. A* **2014**, *481*, 49–53; b) E. De Jong, T. Vijlbrief, R. Hijkoop, G. J. M. Gruter, J. C. van der Waal, *Biomass Bioenergy* **2012**, *36*, 151–159.
[11] X. L. Li, K. Zhang, S. Y. Chen, C. Li, F. Li, H. J. Xu, Y. Fu, *Green Chem.* **2018**, *20*, 1095–1105.
[12] a) Q. Hou, X. Qi, M. Zhen, H. Qian, Y. Nie, C. Bai, S. Zhang, X. Bai, M. Ju, *Green Chem.* **2021**, *23*, 119–231; b) C. Xu, E. Paone, D. Rodríguez-Padrón, R. Luque, F. Mauriello, *Chem. Soc. Rev.* **2020**, *49*, 4273–4306.
[13] a) I. Delidovich, P. J. C. Hausoul, L. Deng, R. Pfüzenreuter, M. Rose, R. Palkovits, *Chem. Rev.* **2016**, *116*, 1540–1599;b) J. He, S. P. Burt, M. Ball, D. Zhao, I. Hermans, J. A. Dumesic, G. W. Huber, *ACS Catal.* **2018**, *8*, 1427–1439.
[14] S. Fulignati, C. Antonetti, D. Licursi, M. Pieraccioni, E. Wilbers, H. J. Heeres, A. M. Raspolli Galletti, *Appl. Catal. A* **2019**, *578*, 122–133.
[15] a) M. Balakrishnan, E. R. Sacia, A. T. Bell, *Green Chem.* **2012**, *14*, 1626–1634; b) K. V. Vikanova, M. S. Chernova, E. A. Redina, G. I. Kapustin, O. P. Tkachenko, L. M. Kustov, *J. Chem. Technol. Biotechnol.* **2021**, *96*, 2421–2425; c) K. V. Vikanova, E. Redina, G. Kapustin, M. Chernova, O. Tkachenko, V. Nissenbaum, L. Kustov, *ACS Sustainable Chem. Eng.* **2021**, *9*, 1161–1171.
[16] a) J. Kim, H. B. Bathula, S. Yun, Y. Jo, S. Lee, J. H. Baik, Y. Suh, *J. Ind. Eng. Chem.* **2021**, *102*, 186–194; b) C. Sarkar, R. Paul, S. C. Shit, Q. T. Trinh, P. Koley, B. S. Rao, A. M. Beale, C. Pao, A. Banerjee, J. Mondal, *ACS Sustainable Chem. Eng.* **2021**, *9*, 2136–2151; c) E. A. Redina, K. V. Vikanova, G. Kapustin, *Russ. J. Phys. Chem. A* **2020**, *94*, 2558–2562; d) K. T. V. Rao, Y. Hu, Z. Yuan, Y. Zhang, X. C. Xu, *Appl. Catal. A* **2021**, *609*, 117892–117903; e) A. J. Kumalaputri, G. Bottari, P. M. Erne, H. J. Heeres, K. Barta, *ChemSusChem* **2014**, *7*, 2266–2275; f) G. Bottari, A. J. Kumalaputri, K. K. Krawczk, B. L. Feringa, H. J. Heeres, K. Barta, *ChemSusChem* **2015**, *8*, 1323–1327.
[17] J. Han, Y. Kim, H. Jang, S. Hwang, J. Jegal, J. W. Kim, Y. Lee, *RSC Adv.* **2016**, *6*, 93394–93397.
[18] D. K. Mishra, H. J. Lee, C. C. Truong, J. Kim, Y. Suh, J. Baek, Y. J. Kim, *J. Mol. Catal.* **2020**, *484*, 110722–110730.
[19] a) I. Elsayed, M. A. Jackson, E. B. Hassan, *Fuel Process. Technol.* **2021**, *213*, 106672–106684; b) J. Han, Y. Kim, B. Y. Jung, S. Y. Hwang, J. Jegal, J. W. Kim, Y. Lee, *Synlett.* **2017**, *28*, 2299–2302; c) M. Musolino, M. J. Ginés-Molina, R. Moreno-Tost, F. Aricò, *ACS Sustainable Chem. Eng.* **2019**, *7*, 10221–10226.
[20] a) D. Hu, H. Hualei, H. Jin, P. Zhang, Y. Hu, S. Ying, X. Li, Y. Yang, J. Zhang, L. Wang, *Appl. Catal. A* **2020**, *590*, 117338–117344;b) D. Gupta, B. Saha, *Catal. Commun.* **2018**, *110*, 46–50;c) M. Shin, J. Kim, Y. Suh, *Appl. Catal. A* **2020**, *603*, 117763–117772.
[21] a) F. Menegazzo, E. Ghedini, M. Signoretto, *Molecules* **2018**, *23*, 2201–2218; b) Y. Zhao, K. Lu, H. Xu, L. Zhu, S. Wang, *Renewable Sustainable Energy Rev.* **2021**, *139*, 110706–110732; c) C. Antonetti, S. Fulignati, D. Licursi, A. M. Raspolli Galletti, *ACS Sustainable Chem. Eng.* **2019**, *7*, 6830–6838; d) C. Antonetti, A. M. Raspolli Galletti, S. Fulignati, D. Licursi, *Catal. Commun.* **2017**, *97*, 146–150.
[22] S. Fulignati, C. Antonetti, E. Wilbers, D. Licursi, H. J. Heeres, A. M. Raspolli Galletti, *J. Ind. Eng. Chem.* **2021**, *100*, 390.e1–390.e9.
[23] R. W. Cargill, *J. Chem. Soc. Faraday Trans. 1* **1978**, *74*, 1444–1456.
[24] Y. Long, Y. Wang, H. Wu, T. Xue, P. Wu, Y. Guan, *RSC Adv.* **2019**, *9*, 25345–25350.
[25] a) T. J. Schwartz, S. D. Lyman, A. H. Motagamwala, M. A. Mellmer, J. A. Dumesic, *ACS Catal.* **2016**, *6*, 2047–2054; b) W. S. Lee, Z. Wang, W. Zheng, D. G. Vlachos, A. Bhan, *Catal. Sci. Technol.* **2014**, *4*, 2340–2352; c) S. A. Zavrrazhnov, A. L. Esipovich, S. Y. Zlobin, A. S. Belousov, A. V. Vorotyntsev, *Catalysts* **2019**, *9*, 231–251.
[26] I. Elsayed, M. A. Jackson, E. B. Hassan, *ACS Sustainable Chem. Eng.* **2020**, *8*, 1774–1785.
[27] N. Perret, A. Grigoropoulos, M. Zanella, T. D. Manning, J. B. Claridge, M. J. Rosseinsky, *ChemSusChem* **2016**, *9*, 521–531.
[28] S. Srivastava, G. C. Jadeja, J. K. Parikh, *Int. J. Chem. React. Eng.* **2018**, *16*, 20170197–20170212.
[29] a) L. Zhang, F. C. Michel Jr, A. C. Co, *Polym. Chem.* **2019**, *57*, 1495–1499; b) L. Guillaume, A. Marshall, N. Niessen, P. Ni, R. M. Gauvin, C. M. Thomas, *Green Chem.* **2021**, *23*, 6931–6935; c) J. Kim, P. H. Hong, K. Choi, G. Moon, J. Kang, S. Lee, S. Lee, H. W. Jung, M. J. Ko, S. W. Hong, *Polymer* **2020**, *12*, 968–978.
[30] R. Barthos, F. Lónyi, G. Onestyák, J. Valyon, *J. Phys. Chem. B* **2000**, *104*, 7311–7319.
[31] R. Le Van Mao, N. Al-Yassir, L. Lu, N. T. Vu, A. Fortier, *Catal.Lett.* **2006**, *112*, 13–18.
[32] a) W. Fang, H. Hu, Z. Ma, L. Wangm, Y. Zhang, *Catalysts* **2018**, *8*, 383–392; b) B. Wozniak, S. Tin, J. G. De Vries, *Chem. Sci.* **2019**, *10*, 6024–6034; c) Z. Xu, P. Yan, W. Xu, X. Liu, Z. Xia, B. Chung, S. Jia, Z. C. Zhang, *ACS Catal.* **2015**, *5*, 788–792.
[33] a) W. Fang, H. Hu, P. Dong, Z. Ma, Y. He, L. Wang, Y. Zhang, *Appl. Catal. A* **2018**, *565*, 146–151; b) H. Hu, D. Hu, H. Jin, P. Zhang, G. Li, H. Zhou, Y. Yang, C. Chen, J. Zhang, L. Wang, *ChemCatChem* **2019**, *11*, 2179–2186.
[34] A. Gelmini, S. Albonetti, F. Cavani, C. Cesari, A. Lolli, V. Zanotti, R. Mazzoni, *Appl. Catal. B* **2016**, *180*, 38–43.
[35] Q. Cao, W. Zhang, S. Luo, R. Guo, D. Xu, *Energy Fuels* **2021**, *35*, 12725–12733.
[36] Q. Cao, J. Guan, G. Peng, T. Hou, J. Zhou, X. Mu, *Catal. Commun.* **2015**, *58*, 76–79.
[37] X. Li, L. Zhang, Q. Deng, S. Chen, J. Wang, Z. Zeng, S. Deng, *ChemSusChem* **2022**, e202102532. Doi:10.1002/cssc.202102532.
[38] H. Hu, T. Xue, Z. Zhang, J. Gan, L. Chen, J. Zhang, F. Qu, W. Cai, L. Wang, *ChemCatChem* **2021**, *13*, 3461–3469.
[39] a) Z. Ma, J. A. Van Bokhoven, *ChemCatChem* **2012**, *4*, 2036–2044; b) B. Tang, S. Li, W. C. Song, Y. Li, E. C. Yang, *Sustain. Energy Fuels* **2021**, *5*, 4724–4735;c) S. He, F. G. H. Klein, T. S. Kramer, A. Chandel, Z. Tegudeer, A. Heeres, H. J. Heeres, *ACS Sustainable Chem. Eng.* **2021**, *9*, 1128–1141.
[40] H. G. Bernal, C. Oldani, T. Funaioli, A. M. Raspolli Galletti, *New J. Chem.* **2019**, *43*, 14694–14700.
[41] a) J. T. Scanlon, D. E. Willis, *J. Chromatogr. Sci.* **1985**, *23*, 333–340; b) A. D. Jorgensen, K. C. Picel, V. C. Stamoudis, *Anal. Chem.* **1990***62*, 683–689; c) T. Holm, *J. Chromatogr. A* **1999***842*, 221–227; d) Y. Kim, K. Kim, J. E. Szulejko, M. Bae, R. J. C. Brown, *Anal. Chim. Acta* **2014**, *830*, 32–41.

Manuscript received: February 1, 2022
Revised manuscript received: March 23, 2022
Accepted manuscript online: April 5, 2022
Version of record online: ■■, ■■■

RESEARCH ARTICLE

From HMF to biofuels: A new cascade process is proposed for the selective synthesis of monomers and biofuels from 5-hydroxymehtylfurfural (HMF) by properly tuning the reaction conditions. In particular, the synthesis of 2,5-bis(ethoxymethyl)tetrahydrofuran (BEMTHF) is studied for the first time, opening the way to the production of a new potential biofuel.

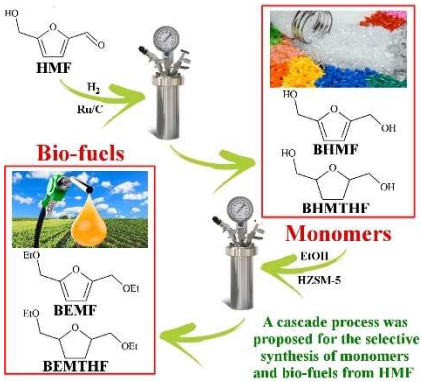

*Dr. S. Fulignati, Prof. C. Antonetti, Dr. T. Tabanelli, Prof. F. Cavani, Prof. A. M. Raspolli Galletti**